Dynamic Modeling of UPFC by Two Shunt Voltage-Source Converters and a Series Capacitor

Farzad Mohammadzadeh Shahir and Ebrahim Babaei

***Abstract*—The unified power flow controller (UPFC) is one of the FACTS devices vastly applied in power systems. This paper presents the modeling of a new structure of UPFC consists of two shunt voltage-source converters and a series capacitor. Through the presented modeling, the transient and steady states responses of UPFC are well investigated. The results of the investigation are presented for the transient and steady states by simulating proposed system in MATLAB changing each system parameter.**

***Index Terms*—FACTS devices, steady state modeling, transient state modeling, UPFC.**

I. Introduction

Stability maintenance is one of the most necessary requisitions of the power system, which has been discussed under several titles such as transient, dynamic, and voltage stability [1]. Recent progresses in high power semiconductor devices and their control techniques fields leads to vast application of FACTS devices in power systems, specially in asymmetric power distribution regulation. UPFC is one of the most important and the most effective FACTS device installed in ac transmission systems [2], [3]. In [4], a new structure, which uses two shunt voltage-source converters along with a capacitor, installed between these converters, is presented for UPFC as shown in Fig. 1 to overcome such problem. The UPFC parameters can be controlled through the capacitor voltage control [4], [5]. Also, the total harmonics distortion (THD) of injected series voltage is decreased in comparison with that of the conventional structures. In addition, the control and measuring systems design is simplified and the insulation and protection levels of transformers are well reduced. In this paper, it is tried to present a dynamic model for the UPFC structure presented in [4], [5] through modeling and mathematical relations calculation as well as stability analysis of this system by investigating the assumed system's critical eigenvalues condition.

II. Mathematical Modeling

A. Voltage Source Converters Modeling

The operation of four input control parameters of the presented UPFC ($\delta_{E,1}$, $\delta_{E,2}$, $m_{E,1}$, and $m_{E,2}$) are introduced and investigated to evaluate its dynamic model. Fig. 2(a) shows the structure of this system in details. The mathematical relations of this structure must be extracted for modeling. In order to achieve this aim, one of the phases is selected and the analyses are carried out for just this phase of shunt voltage-source converters due to the similarity of the structures and performance of the converters. For further explanations, Fig. 2(b), which shows the UPFC components such as dc link, a phase of exciting transformer in shunt voltage-source converter 1, and its related leg is initially considered. Here, it is assumed that C_{dc}, dc link capacitor, is divided into two equal parts and its middle point is named as *n*. In addition, installed switch, $\xi_{E,1,a}$ and $\xi'_{E,1,a}$ switches are bidirectional ones with r_s on resistance, which can be considered as the conduction losses parameter of the switches and can be applied in losses analysis. The switches $S_{E,1,a}$ and $S'_{E,1,a}$ which define positive and negative switching function, respectively, have two operation modes for on/off states. According to the PWM technique application [6], for voltage-source converter operation control, $S_{E,1,a}$ and $S'_{E,1,a}$ are always complementary and the following is valid:

$$S_{E,1,a} + S'_{E,1,a} = 1 \quad (1)$$

The following is obtained applying Kirchhoffs' voltage law on the circuit of Fig. 2(b):

$$L_{E,1,a}\frac{di_{E,1,a}}{dt} + r_{E,1,a}i_{E,1,a} = v_{Et,1,a} - v_{E,1,a} \quad (2)$$

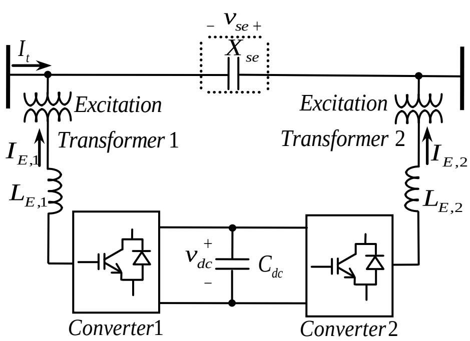

Fig. 1. Structure of presented UPFC in [4]

In (2), $L_{E,g,k}$, $i_{E,g,k}$, $r_{E,g,k}$, $v_{Et,g}$, $v_{E,g}$ are used for leakage inductance of transformer, current in shunt converter, resistance of transformer, voltage of shunt

Manuscript received March 17, 2013; revised May 6, 2013.

Farzad Mohamamdzadeh Shahir is with Faculty of Electrical and Computer Engineering, University of Tabriz, Tabriz, Iran (e-mail: f-mohammadzadeh@iau-ahar.ac.ir, f.m.shahir@gmail.com).

Ebrahim Babaei is with Faculty of Electrical and Computer Engineering, University of Tabriz, Tabriz, Iran (e-mail: e-babaei@tabrizu.ac.ir).

DOI: 10.7763/IJCEE.2013.V5.757

converter, and injecting voltage of shunt converter, respectively, on converter g and phase k which g and k subscripts refer to number of shunt converter, and phase of three phase system, respectively. The following is obtained according to Fig. 2(b):

$$v_{E,1,a} = v_{FH} + v_{Hn} \tag{3}$$

Parameter v_{FH} can be calculated on a period as follows:

$$v_{FH} = (i_{E,1,a} r_S + v_{dc}) S_{E,1,a} + i_{E,1,a} r_S S'_{E,1,a} \tag{4}$$

In (4), v_{dc} is the voltage of dc link. Applying $S'_{E,1,a}$ value from (1) to (4) leads to the follows:

$$v_{FH} = v_{dc} S_{E,1,a} + i_{E,1,a} r_S \tag{5}$$

Considering (3) and (5), $v_{E,1,a}$ is obtained as follows:

$$v_{E,1,a} = v_{dc} S_{E,1,a} + i_{E,1,a} r_S + v_{Hn} \tag{6}$$

From (2) and (6) and assuming $R_{E,1,a} = r_S + r_{E,1,a}$ the following can be obtained:

$$L_{E,1,a} \frac{di_{E,1,a}}{dt} = -R_{E,1,a} i_{E,1,a} - (v_{dc} S_{E,1,a} + v_{Hn}) + v_{Et,1,a} \tag{7}$$

According to Fig. 2(a) and assuming the system balance, parameter v_{Hn} could be calculated as follows:

$$v_{Hn} = -\left(\frac{v_{dc}}{3}\right) \sum_{k=a,b,c} S_{E,1,k} \tag{8}$$

If $S_{E,1,a}$ is expanded by Fourier discrete series [7-10], the following is valid:

$$\bar{d}_{E,1,a} = \frac{m_{E,1}}{2} \cos(\omega t - \delta_{E,1}) + \frac{1}{2} \tag{9}$$

In (9), $\bar{d}_{E,g,k}$, $\delta_{E,g}$, and $m_{E,g}$ are mean positive half Switching function, phase angle, and modulation index of shunt converter g, respectively. Therefore, v_{Hn} in (9) is obtained from $\bar{d}_{E,1,a}$, $\bar{d}_{E,1,b}$ and $\bar{d}_{E,1,c}$ applying proper values of $S_{E,1,k}$ (for *k= a, b, and c*). Applying v_{Hn} from (9) and v_{FH} from (5) in (3) results:

$$v_{E,1,a} = A_{E,1} \cos\delta_{E,1} = \frac{m_{E,1} v_{dc}}{2} \cos(\omega t + \delta_{E,1}) \tag{10}$$

In (10), $A_{E,g}$ is voltage amplitude. Finally, the relation obtained for phase a and assuming same switch ($R_{E,1,a} = R_{E,1,b} = R_{E,1,c} = R_{E,1}$ and $L_{E,1,a} = L_{E,1,b} = L_{E,1,c} = L_{E,1}$), is achieved applying $v_{E,1,a}$ value of (10) in (2) as follows :

$$L_{E,1} \frac{di_{E,1,a}}{dt} = -R_{E,1} i_{E,1,a} - A_{E,1} \cos\delta_{E,1} + v_{Et,1,a} \tag{11}$$

The obtained mathematical model for phase *a*, in (11) can be acceptable for phase *b* and *c* with considering 120° and 240° phase difference, respectively. Also, in this analysis, the equations are obtained for shunt converter 1 can be acceptable for three phase of shunt converter 2 as follows:

$$L_{E,2} \frac{di_{E,2,a}}{dt} = -R_{E,2} i_{E,2,a} - A_{E,2} \cos\delta_{E,2} + v_{Et,2,a} \tag{12}$$

B. DC Link Modeling

In order to dynamic modeling of dc link, the following equations can be considered:

$$i_{dc} = i_{E,1,dc} + i_{E,2,dc} = \sum_{k=a,b,c} \left(i_{E,1,k} \bar{d}_{E,1,k} + i_{E,2,k} \bar{d}_{E,2,k} \right) \tag{13}$$

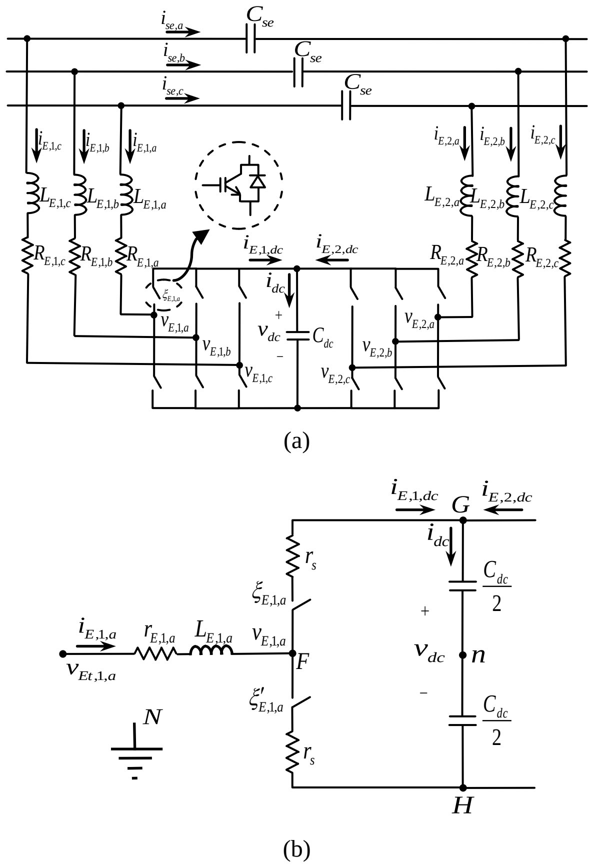

Fig. 2. Equivalent circuit of the proposed UPFC; (a) Detailed structure; (b) Equivalent circuit of phase *a*

Applying $\bar{d}_{E,1,k}$ (for *k=a, b, and c*) from (9) and $\bar{d}_{E,2,k}$, the following is obtained for i_{dc} value:

$$i_{dc} = \frac{m_{E,1}}{2} [\cos(\omega t + \delta_{E,1}) \;\; \cos(\omega t + \delta_{E,1} - 120^\circ) \;\; \cos(\omega t + \delta_{E,1} + 120^\circ)] \times \begin{bmatrix} i_{E,1,a} \\ i_{E,1,b} \\ i_{E,1,c} \end{bmatrix} + \frac{m_{E,1}}{2} [\cos(\omega t + \delta_{E,2}) \;\; \cos(\omega t + \delta_{E,2} - 120^\circ) \;\; \cos(\omega t + \delta_{E,2} + 120^\circ)] \times \begin{bmatrix} i_{E,2,a} \\ i_{E,2,b} \\ i_{E,2,c} \end{bmatrix}. \tag{14}$$

C. Series Capacitor Modeling

Here, it is intended to model the series capacitor as follow:

$$\frac{dv_{se,k}}{dt}=\frac{1}{C_{se}}i_{se,k} \quad for \;\; k=a,b,c \tag{15}$$

The series capacitor current, i_{se} , is considered as follows:

$$i_{se,k}=C_{se}\left(\frac{dv_{Et,2,k}}{dt}-\frac{dv_{Et,1,k}}{dt}\right) \quad for \;\; k=a,b,c \tag{16}$$

In the aforementioned equations, C_{se} and $v_{se,k}$ show series capacitor and its voltage. Applying i_{se} from (16) in (15) results in capacitor dynamic equation as follows:

$$\frac{dv_{se,k}}{dt}=\frac{dv_{Et,2,k}}{dt}-\frac{dv_{Et,1,k}}{dt} \quad for \;\; k=a,b,c \tag{17}$$

D. The Complete Equivalent Circuit of the Proposed UPFC

Based on (11), (12), (14), and (17), the complete equivalent circuit of the proposed UPFC can be shown as the structure illustrated in Fig. 3.

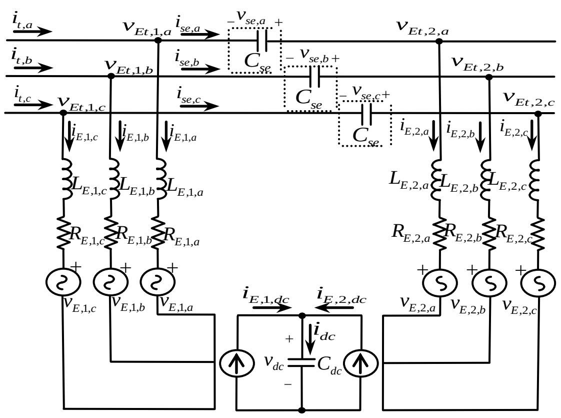

Fig. 3. Generalized equivalent circuit of the proposed UPFC

III. State Space Equations Derivation

Based on (11), (12), (14), and (17), the state space equations of the proposed UPFC can be expressed as follows:

$$\dot{X}=AX+BU \tag{18}$$

where X and U are considered as follows:

$$X=[i_{E,1,a} \quad i_{E,1,b} \quad i_{E,1,c} \quad i_{E,2,a} \quad i_{E,2,b} \quad i_{E,3,c} \quad v_{dc} \quad v_{se}]^T$$
$$U=[v_{Et,1,a} \quad v_{Et,1,b} \quad v_{Et,1,c} \quad v_{Et,2,a} \quad v_{Et,2,b} \quad v_{Et,2,c}]^T$$

The non-zero arrays of A and B values are presented in appendix. It should be noted that the mathematical model derived for the proposed UPFC is valid for the angular frequency domain less than the switching frequency f_s .

IV. Steady State Model

In this section, the losses of UPFC structure are neglected. The dc link voltage supporting shunt voltage-source converters 1 and 2 is considered constant. The following can be obtained for the steady state equations of three-phase system from Fig. 2, applying KVL, and neglecting the resistance of transformers due to great values of the leakage reactance:

$$\bar{V}_{Et,g,k}=jX_{E,1}\bar{I}_{E,g,k}+\bar{V}_{E,g,k} \quad for \;\; k=a,b,c \;\; g=1,2 \tag{19}$$

Considering Fig. 2, the following is valid for the voltage magnitude of the series capacitor:

$$\bar{V}_{se,k}=-jX_{se}\bar{I}_{se,k}=\bar{V}_{Et,2,k}-\bar{V}_{Et,1,k} \quad for \;\; k=a,b,c \tag{20}$$

According to (19) and (20), the final steady state model of this structure would be as follows:

$$\begin{bmatrix} -Z_{E,1} & & & & & \\ & -Z_{E,1} & & & & \\ & & -Z_{E,1} & & & \\ & & & -Z_{E,2} & & \\ & & & & -Z_{E,2} & \\ & & & & & -Z_{E,2} \end{bmatrix}\begin{bmatrix} I_{E,1,a} \\ I_{E,1,b} \\ I_{E,1,c} \\ I_{E,2,a} \\ I_{E,2,b} \\ I_{E,2,c} \end{bmatrix}+\begin{bmatrix} V_{Et,1,a}-V_{E,1,a} \\ V_{Et,1,b}-V_{E,1,b} \\ V_{Et,1,c}-V_{E,1,c} \\ V_{Et,2,a}-V_{E,2,a} \\ V_{Et,2,b}-V_{E,2,b} \\ V_{Et,2,c}-V_{E,2,c} \end{bmatrix}=0 \tag{21}$$

where $Z_{E,1}$, $Z_{E,2}$, $V_{E,1,k}$, and $V_{E,2,k}$ are as follows:

$$Z_{E,g}=R_{E,g}+j\omega L_{E,g} \quad for \;\; g=1,2$$

$$V_{E,g,k}=\frac{M_{E,g}V_{dc}}{2\sqrt{2}}\angle\delta_{E,g} \quad for \;\; g=1,2 \;\; and \;\; k=a,b,c$$

Based on (21), the steady state single line diagram of assumed UPFC can be considered as Fig. 4. The constraint shown in this figure ($P_{E,1}+P_{E,2}=0$) is due to the following facts, (a). the series capacitor voltage directly depends on the voltage magnitude and the performance of 1 and 2 shunt converters and its reactive power is determined by the voltage ratio of converter 2 to converter 1; (b). The dc link voltage is constant if no active power is exchanged and losses are neglected; (c). The operation of converters mutually depends on each other.

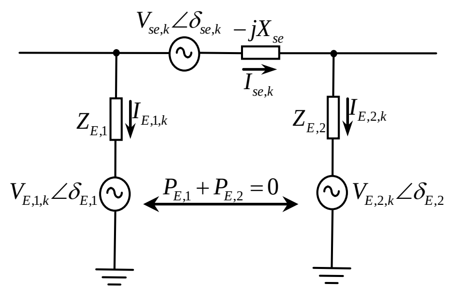

Fig. 4. Steady state model of the proposed UPFC

V. Dynamic Model

The dc link voltage on d-q axis is considered as follows applying Park's transformation:

$$\frac{dv_{dc}}{dt} = \frac{3m_{E,1}}{4C_{dc}}\left[\cos\delta_{E,1}\ \ \sin\delta_{E,1}\right]\begin{bmatrix} i_{E,1,d} \\ i_{E,1,q}\end{bmatrix} + \frac{3m_{E,2}}{4C_{dc}}\left[\cos\delta_{E,2}\ \ \sin\delta_{E,2}\right]\begin{bmatrix} i_{E,2,d} \\ i_{E,2,q}\end{bmatrix}. \quad (22)$$

The followings are valid for the injecting voltages of 1 and 2 converters terminal on d-q axis:

$$\begin{bmatrix} v_{Et,g,d} \\ v_{Et,g,q}\end{bmatrix} = \begin{bmatrix} 0 & -X_{E,g} \\ 0 & X_{E,g}\end{bmatrix}\begin{bmatrix} i_{E,g,d} \\ i_{E,g,q}\end{bmatrix} + \begin{bmatrix} \frac{m_{E,g} v_{dc}}{2}\cos\delta_{E,g} \\ \frac{m_{E,g} v_{dc}}{2}\sin\delta_{E,g}\end{bmatrix} \quad for\ g = 1,2. \quad (23)$$

The series capacitor voltage can be expressed as follows:

$$\begin{bmatrix} v_{se,d} \\ v_{se,q}\end{bmatrix} = \begin{bmatrix} v_{Et,1,d} - v_{Et,2,d} \\ v_{Et,1,q} - v_{Et,2,q}\end{bmatrix} \quad (24)$$

Considering (23) and (24), the state variables are as follows:

$$\dot{x}_{dqo} = A_{dqo} x_{dqo} + B_{dqo} u_{dqo} \quad (25)$$

where x_{dqo} and u_{dqo} are as follows:

$$x_{dqo} = [i_{E,1,d}\ \ i_{E,1,q}\ \ i_{E,1,o}\ \ i_{E,2,d}\ \ i_{E,2,q}\ \ i_{E,2,o}\ \ v_{dco}\ \ v_{seo}]^T$$
$$u_{dqo} = [v_{Et,1,d}\ \ v_{Et,1,q}\ \ v_{Et,1,o}\ \ v_{Et,2,d}\ \ v_{Et,2,q}\ \ v_{Et,2,o}]^T$$

where A_{dqo} and B_{dqo} are explained in appendix.

VI. Small Signal Dynamic Model

Based on d-q axis small signal model of proposed UPFC (25) is linearized by making an approximation around the system operation point, and is expressed as follows:

$$\Delta\dot{x}_{dqo} = A'_{dqo}\Delta x_{dqo} + B'_{dqo}\Delta u_{dqo} \quad (26)$$

The non-zero arrays of A'_{dqo} and B'_{dqo} are presented in appendix. The small signal model presented in (26) can easily be applied in a wide range of system dynamics investigations such as low frequency electromechanical modes (0.1Hz-2Hz), tensional oscillatory modes (5-55Hz), and 2nd and 3rd order resonance harmonics.

VII. Simulation Results

The effects of each UPFC parameters variation are investigated and simulated in MATLAB software. Here, the UPFC parameters are considered as $X_{E,1} = X_{E,2} = 0.3pu$, $m_{E,1} = m_{E,2} = 1$, $R_{E,1} = R_{E,2} = 0.3pu$, $v_{dc} = 2pu$, $X_{se} = 0.2$, $C_{dc} = 3pu$, $f_s = 50Hz$.

A. Transient State Investigation

In this subsection, the system's dynamic stability is investigated through system's critical eigenvalues analysis. Due to the simulation results, the $\delta_{E,1}$ variations do not improve the system's critical eigenvalues and transient state stability parameters and does not affect the dynamic stability of the presented UPFC. The simulation results are shown in Fig. 5. Due to the simulation results, the $\delta_{E,2}$ variations improve the system's critical eigenvalues and transient state stability parameters.

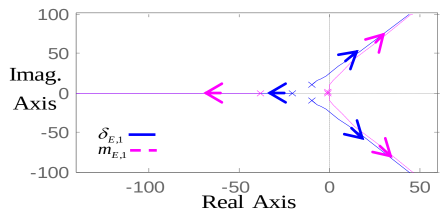

(a)

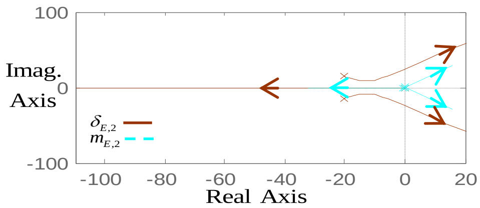

(b)

Fig. 5. Eigenvalues variation, (a) $\delta_{E,1}$ and $m_{E,1}$, (b) $\delta_{E,2}$ and $m_{E,2}$

B. Steady State Investigation

The variations of $|I_{E,1}|$ and $|I_{E,2}|$ are investigated in this subsection. Parameter $|V_{se}|$ is considered to be constant and to be equal to 0.5pu and it is assumed that $|V_{E,1}|$ and $|V_{E,2}|$ varies from 0.9pu to 1.2pu and $\delta_{E,2}$ and $\delta_{E,1}$ varies in rectifying to alternating modes between -45^o and $+45^o$, respectively. according to Fig. 6(a), the magnitude of $|I_{E,1}|$ is maximum in $\delta_{E,2} = 0^\circ$ and decreases as $\delta_{E,2}$ varies for converter 2 operation change to rectifying, and for constant $\delta_{E,2}$ value, the magnitude of $|I_{E,1}|$ decreases as $|V_{E,1}|$ magnitude increases. According to simulation results are shown in Fig. 6(b), the magnitude of $|I_{E,2}|$ is maximum in $\delta_{E,1} = 0^\circ$ and decreases as $\delta_{E,1}$ varies for converter 1 operation change to rectifying and for constant $\delta_{E,1}$ value, the magnitude of $|I_{E,2}|$ decreases as $|V_{E,2}|$ magnitude increases.

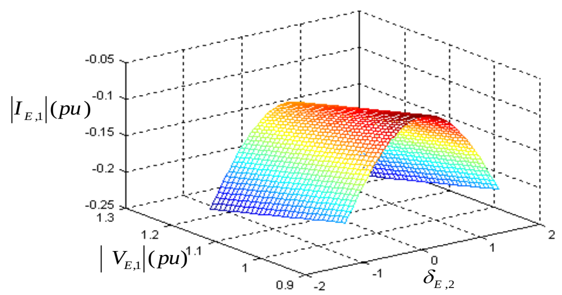

(a)

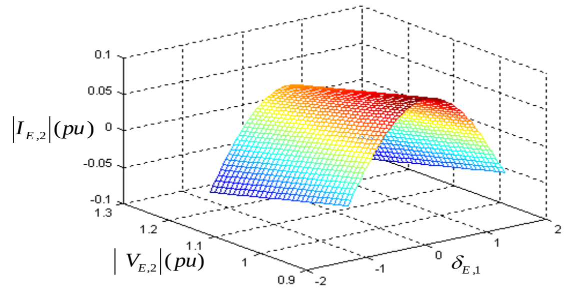

(b)

Fig. 6. (a) $|I_{E,1}|$ variations, (b) $|I_{E,2}|$ variations ($|V_{se}| = 0.5pu$)

VIII. Conclusion

In this paper, a generalized mathematical model is presented for the proposed UPFC. The presented modeling can be applied in power flow calculations, system's eigenvalues condition assess, and dynamic and transient states stability analysis. In this modeling, it is assumed that the system is symmetric and the three-phase operation is balance. Steady transient states and the considered UPFC small signal equations are derived in details. The transient state equations are presented in linear mode around system's operation point. In this paper, the steady state and the transient state are investigated separately. In addition, the effect of each UPFC parameter variation in steady state mode is expressed and can be applied in power flow investigations. According to the simulation results, $|I_{E,2}|$ intensively affects $|V_{se}|$, active and reactive powers, and UPFC performance. In transient state evaluation, the effects of control parameters variation of this structure on the considered UPFC and its variations on the system's eigenvalues are assessed and $\delta_{E,2}$ reduction desirably improves the transient state stability.

Appendix

The non-zero arrays of matrix A, in (18) are as follows:

$$a_{g,11} = a_{g,22} = a_{g,33} = -\frac{R_{E,1}}{L_{E,1}}, a_{g,44} = a_{g,55} = a_{g,66} = -\frac{R_{E,2}}{L_{E,2}}$$

$$a_{g,17} = s_1 \cos(\omega t + \delta_{E,1}), a_{g,17} = s_1 \cos(\omega t + \delta_{E,1} - 120^\circ)$$

$$a_{g,37} = s_1 \cos(\omega t + \delta_{E,1} + 120^\circ), a_{g,47} = s_2 \cos(\omega t + \delta_{E,2})$$

$$a_{g,57} = s_2 \cos(\omega t + \delta_{E,2} - 120^\circ),$$
$$a_{g,67} = s_2 \cos(\omega t + \delta_{E,2} + 120^\circ)$$

$$a_{g,71} = s_3 \cos(\omega t + \delta_{E,1}), a_{g,72} = s_3 \cos(\omega t + \delta_{E,1} - 120^\circ)$$

$$a_{g,73} = s_3 \cos(\omega t + \delta_{E,1} + 120^\circ), a_{g,74} = s_4 \cos(\omega t + \delta_{E,2})$$

$$a_{g,75} = s_4 \cos(\omega t + \delta_{E,2} - 120^\circ),$$
$$a_{g,76} = s_4 \cos(\omega t + \delta_{E,2} + 120^\circ)$$

The non-zero arrays of Matrix B, in (18) are as follows:

$$b_{g,11} = b_{g,22} = b_{g,33} = \frac{1}{L_{E,1}},$$

$$b_{g,44} = b_{g,55} = b_{g,66} = \frac{1}{L_{E,2}}, b_{g,88} = \frac{1}{C_{se}}$$

$$b_{g,77} = \frac{1}{C_{dc}},$$

$$b_{g,81} = b_{g,82} = b_{g,83} = -b_{g,84} = -b_{g,85} = -b_{g,86} = -1$$

The non-zero arrays of matrix A_{dqo}, in (25) are as follows:

$$a_{dq0,11} = a_{dq0,22} = -\frac{R_{E,1}}{L_{E,1}}, \quad a_{dq0,33} = a_{dq0,44} = -\frac{R_{E,2}}{L_{E,2}}$$

$$a_{dq0,12} = -a_{dq0,21} = -a_{dq0,43} = a_{dq0,34} = \omega_0,$$
$$a_{dq0,35} = s_6 \cos\delta_{E,2}$$

$$a_{dq0,15} = s_5 \cos\delta_{E,1}, a_{dq0,25} = s_5 \sin\delta_{E,1}, a_{dq0,45} = s_6 \sin\delta_{E,2}$$

$$a_{dq0,52} = s_7 \sin\delta_{E,1}, a_{dq0,53} = s_8 \cos\delta_{E,2}, a_{dq0,51} = s_7 \cos\delta_{E,1}$$

$$a_{g,27} = -s_8 \cos(\omega t + \delta_{E,1} - 120^\circ)$$

The non-zero arrays of matrix B_{dqo}, in (25) are as follows:

$$b_{dq0,11} = b_{dq0,22} = \frac{1}{L_{E,1}}, b_{dq0,33} = b_{dq0,44} = \frac{1}{L_{E,2}},$$
$$b_{dq0,55} = \frac{1}{C_{dc}}$$

$$b_{dq0,61} = b_{dq0,62} = -b_{dq0,63} = -b_{dq0,64} = -1, b_{dq0,66} = \frac{1}{C_{se}}$$

The non-zero arrays of matrix A'_{dqo}, in (26) are as follows:

$$a'_{dq0,11} = a'_{dq0,22} = -\frac{R_{E,1}\omega_0}{L_{E,1}}, a'_{dq0,33} = a'_{dq0,44} = -\frac{R_{E,2}\omega_0}{L_{E,2}}$$

$$a'_{dq0,12} = -a'_{dq0,21} = a'_{dq0,34} = -a'_{dq0,43} = \omega_0$$

$$a'_{dq0,15} = -s_9 \cos\delta_{E,1}, a'_{dq0,25} = -s_9 \sin\delta_{E,1},$$
$$a'_{dq0,35} = s_{10} \cos\delta_{E,2}$$

$$a'_{dq0,45} = s_{10} \sin\delta_{E,2}, a'_{dq0,51} = s_{11} \cos\delta_{E,1}, a'_{dq0,52} = s_{11} \sin\delta_{E,1}$$

$$a'_{dq0,53} = s_{12} \cos\delta_{E,2}, a'_{dq0,54} = s_{12} \sin\delta_{E,2}$$

$$a'_{dq0,63} = -a'_{dq0,64} = \omega_0 L_{E,2}, a'_{dq0,61} = -a'_{dq0,62} = -\omega_0 L_{E,1}$$

$$a'_{dq0,65} = 0.5\left(m_{E,2}\sin\delta_{E,2} - m_{E,1}\sin\delta_{E,1}\right) + 0.5\left(m_{E,1}\cos\delta_{E,1} - m_{E,2}\cos\delta_{E,2}\right)$$

The non-zero arrays of matrix B'_{dqo}, in (26) are as follows:

$$b'_{dq0,11} = -s_{13}\cos\delta_{E,1}, b'_{dq0,12} = s_9 \sin\delta_{E,1},$$
$$b'_{dq0,21} = -s_{13}\sin\delta_{E,1}$$

$$b'_{dq0,22} = -s_9 \cos\delta_{E,1},\ b'_{dq0,33} = s_{14}\cos\delta_{E,2},\ b'_{dq0,34} = -s_{10}\sin\delta_{E,2}$$

$$b'_{dq0,43} = s_{14}\sin\delta_{E,2},\ b'_{dq0,44} = s_{10}\cos\delta_{E,2}$$

$$b'_{dq0,51} = s_{15}(i_{E,1,d}\cos\delta_{E,1} + i_{E,1,q}\sin\delta_{E,1})$$

$$b'_{dq0,52} = -s_{15}m_{E,1}(i_{E,1,d}\sin\delta_{E,1} - i_{E,1,q}\cos\delta_{E,1})$$

$$b'_{dq0,53} = -s_{15}(i_{E,2,d}\cos\delta_{E,2} + i_{E,2,q}\sin\delta_{E,2})$$

$$b'_{dq0,54} = s_{15}m_{E,2}(i_{E,2,d}\sin\delta_{E,2} - i_{E,2,q}\cos\delta_{E,2})$$

$$b'_{dq0,61} = 0.5v_{dc}\left(\cos\delta_{E,1} + \sin\delta_{E,1}\right)$$

$$b'_{dq0,62} = 0.5v_{dc}\left(\sin\delta_{E,2} + \cos\delta_{E,2}\right)$$

$$b'_{dq0,63} = 0.5v_{dc}m_{E,1}\left(\sin\delta_{E,1} - \cos\delta_{E,1}\right)$$

$$b'_{dq0,64} = 0.5v_{dc}m_{E,2}\left(\cos\delta_{E,2} - \sin\delta_{E,2}\right)$$

$$s_1 = -\left(\frac{m_{E,1}}{2L_{E,1}}\right),\ s_2 = \left(\frac{m_{E,2}}{2L_{E,2}}\right),\ s_3 = \left(\frac{m_{E,1}}{2C_{dc}}\right),\ s_4 = \left(\frac{m_{E,4}}{2C_{dc}}\right)$$

$$s_5 = \left(\frac{m_{E,1}}{2L_{E,1}}\right),\ s_6 = \left(\frac{m_{E,2}}{2L_{E,2}}\right),\ s_7 = \left(\frac{3m_{E,1}}{4C_{dc}}\right),\ s_8 = \left(\frac{3m_{E,2}}{4C_{dc}}\right)$$

$$s_9 = \left(\frac{\omega_0 m_{E,1}}{2L_{E,1}}\right),\ s_{10} = \left(\frac{\omega_0 m_{E,2}}{2L_{E,2}}\right),\ s_{11} = \left(\frac{\omega_0 m_{E,1}}{2C_{dc}}\right),\ s_{12} = \left(\frac{\omega_0 m_{E,2}}{2C_{dc}}\right)$$

$$s_{13} = \left(\frac{\omega_0 v_{dc}}{2L_{E,1}}\right),\ s_{14} = \left(\frac{\omega_0 v_{dc}}{2L_{E,2}}\right),\ s_{15} = \left(\frac{\omega_0}{2C_{dc}}\right)$$

REFERENCES

[1] P. Kndor, *Power system stability and control*, Mc. Graw Hill, New York, 1994.

[2] N. G. Higorani and L. Gyugyi, *Understanding FACTS: concepts and technology of flexible ac transmission systems*, IEEE Press, New Jersey, 1999.

[3] F. M. Shahir, E. Babaei, S. Ranjbar, and S. Torabzad, “New Control Methods for Matrix Converter based UPFC under Unbalanced Load,” in *Proc. IICPE*, 2012.

[4] A. K. Sdigh, M. T. Hagh, and M. Sabahi, “Unified power flow controller based on two shunt converters and a series capacitor,” *Elsevier Journal of Electric Power System Research*, 2010, vol. 80, no. 2, pp. 1511-1519.

[5] F. M. Shahir and E. Babaei, “Dynamic Modeling of UPFC by Two Shunt Voltage-Source Converters and a Series Capacitor,” in *Proc. ICECT*, 2012, pp. 554-558.

[6] B. Mwinyiwiwa, Z. Wolanski, and B. T. Ooi, “Current equalization in SPWM FACTS controllers at lowest switching rates,” *IEEE Trans. Power Electron.*, 1999, vol. 14 , no. 5, pp. 900-905.

[7] F. M. Shahir and E. Babaei, “Evaluating the Dynamic Stability of Power System Using UPFC based on Indirect Matrix Converter,” in *Proc. ICECT*, 2012, pp. 548-553.

[8] R. H. Adware, P. P. Jagtap, and J. B. Helonde, “Power system oscillations damping using UPFC damping controller,” in *Proc. ICETET*, 2010, pp. 340-344.

[9] F. M. Shahir, E. Babaei, S. Ranjbar, and S. Torabzad, “Dynamic Modeling of UPFC based on Indirect Matrix Converter,” *in Proc. IICPE*, 2012.

[10] F. M. Shahir and E. Babaei, “Evaluation of Power System Stability by UPFC via Two Shunt Voltage-Source Converters and a Series Capacitor,” in *Proc. ICEE*, 2012.

Farzad Mohammadzadeh Shahir was born in Tabriz, Iran, in 1985. He received the B.S. degree in electronic engineering from Islamic Azad University, Mianeh, Iran, the M.S. degree in electrical engineering from Islamic Azad University, Ahar, Iran, in 2008 and 2011, respectively.

In 2004, he joined the Iran Tractor Manufacturing Company, Tabriz, Iran, where he has been an electrical engineering in there. His current research interests include power system dynamic and power electronic converters.

Ebrahim Babaei was born in Ahar, Iran in 1970. He received his B.S. and M.S. in Electrical Engineering from the Department of Engineering, University of Tabriz, Tabriz, Iran, in 1992 and 2001, respectively, graduating with first class honors. He received his Ph.D. in Electrical Engineering from the Department of Electrical and Computer Engineering, University of Tabriz, Tabriz, Iran, in 2007. In 2004, he joined the Faculty of Electrical and Computer Engineering, University of Tabriz. He was an Assistant Professor from 2007 to 2011 and has been an Associate Professor since 2011. He is the author of more than 170 journal and conference papers. His current research interests include the analysis and control of power electronic converters, matrix converters, multilevel converters, FACTS devices, power system transients, and power system dynamics.